Journal of Orthopaedic Research 23 (2005) 67–76

Journal of Orthopaedic Research

www.elsevier.com/locate/orthres

Viscoelastic properties of the human medial collateral ligament under longitudinal, transverse and shear loading

Carlos Bonifasi-Lista [a], Spencer P. Lake [a], Michael S. Small [a], Jeffrey A. Weiss [a,b,*]

[a] Department of Bioengineering, University of Utah, 50 S Central Campus Drive, Rm. 2480, Salt Lake City, UT 84112, USA

[b] Department of Orthopedics, University of Utah, 30 North 1900 East, Rm. 3B165, Salt Lake City, UT 84132, USA

Received 9 June 2004

Abstract

Ligament viscoelasticity controls viscous dissipation of energy and thus the potential for injury or catastrophic failure. Viscoelasticity under different loading conditions is likely related to the organization and anisotropy of the tissue. The objective of this study was to quantify the strain- and frequency-dependent viscoelastic behavior of the human medial collateral ligament (MCL) in tension along its longitudinal and transverse directions, and under shear along the fiber direction. The overall hypothesis was that human MCL would exhibit direction-dependent viscoelastic behavior, reflecting the composite structural organization of the tissue. Incremental stress relaxation testing was performed, followed by the application of small sinusoidal strain oscillations at three different equilibrium strain levels. The peak and equilibrium stress–strain curves for the longitudinal, transverse and shear tests demonstrate that the instantaneous and long-time stress–strain response of the tissue differs significantly between loading conditions of along-fiber stretch, cross-fiber stretch and along-fiber shear. The reduced relaxation curves demonstrated at least two relaxation times for all three test modes. Relaxation resulted in stresses that were 60–80% of the initial stress after 1000 s. Incremental stress relaxation proceeded faster at the lowest strain level for all three test configurations. Dynamic stiffness varied greatly with test mode and equilibrium strain level, and showed a modest but significant increase with frequency of applied strain oscillations for longitudinal and shear tests. Phase angle was unaffected by strain level (with exception of lowest strain level for longitudinal samples) but showed a significant increase with increasing strain oscillation frequency. There was no effect of test type on the phase angle. The increase in phase and thus energy dissipation at higher frequencies may protect the tissue from injury at faster loading rates. Results suggest that the long-time relaxation behavior and the short-time dynamic energy dissipation of ligament may be governed by different viscoelastic mechanisms, yet these mechanisms may affect tissue viscoelasticity similarly under different loading configurations.

Keywords: Viscoelasticity; Ligament; Material properties; Shear; MCL

Introduction

Ligaments possess both anisotropic and viscoelastic material properties. Material anisotropy is primarily a result of local collagen orientation, resulting in direction-dependent material properties that are often described as transversely isotropic [18,35,45,46]. In contrast, there is little agreement in the literature as to the mechanisms governing ligament viscoelasticity. An improved understanding of ligament viscoelasticity can help to interpret the role of different tissue components in the observed material behavior, thus providing a means to describe alterations in tissue ultrastructural organization and function in injury and disease. Further, the role of viscous dissipation in modulating the potential for injury can be elucidated.

Ligament viscoelasticity under uniaxial tensile loading has been attributed to a number of mechanisms. These include inherent viscoelasticity of the collagen fibers [38], the extracellular matrix [45], interfibrillar crosslinking [31,34,36], collagen intermolecular crosslinking [4,12,21,34], and fluid content [7] and movement within and in/out of the tissue during loading [2,6]. Collagen interfibrillar crosslinks consist of soluble interfibrillar carbohydrate-rich polymers (anionic

* Corresponding author. Address: Department of Bioengineering, University of Utah, 50 S Central Campus Drive, Rm. 2480 Salt Lake City, UT 84112, USA. Tel.: +1-801-587-7833; fax: +1-801-585-5361.

E-mail address: jeff.weiss@utah.edu (J.A. Weiss).

0736-0266/$ - see front matter
doi:10.1016/j.orthres.2004.06.002

glycosaminoglycan chains of proteoglycan molecules [9,39]). These interfibrillar crosslinks may contribute to both the elastic and viscoelastic material properties of ligaments and tendons under tensile, shear and compressive loading [9,36,39]. Collagen intermolecular crosslinking involves both a precise enzymatically controlled crosslinking during development and maturation and a nonenzymatic mechanism following maturation of the tissue [3,21]. The exact sources of ligament viscoelasticity under different loading conditions remain controversial.

Material anisotropy implies a directional dependence in the response to applied loading. This suggests that the viscoelastic response depends on the direction of applied load. With few exceptions [45,46], experimental studies of ligament viscoelasticity have examined only the uniaxial tensile behavior along a direction aligned with the collagen fibers. Although many ligaments experience primarily tensile strains in vivo, shear and transverse deformations also occur. These modes of deformation can become extreme without necessarily damaging the collagen fibers. However, disruption of fibril crosslinks or the extrafibrillar matrix may not present clinically as a tear.

The objective of this study was to characterize the direction-dependent viscoelasticity of ligament under tensile tests along the local fiber direction, tensile tests transverse to the fiber direction, and shear loading along the fiber direction. The human medial collateral ligament (MCL) was chosen for study because of the high incidence of MCL injuries [28] and the clinical importance of the MCL in restraining valgus rotations. Further, it is a relatively planar structure that experiences large variations in strain during normal and abnormal loading in vivo [19,23]. The overall hypothesis of the study was that the human MCL exhibits direction-dependent viscoelastic behavior, reflecting the composite structural organization of the tissue.

Methods

Experimental procedures were designed to determine the effects of frequency of strain oscillation, strain level and specimen orientation on ligament viscoelasticity. Small sinusoidal strain oscillations about an equilibrium strain allow the application of linear viscoelastic theory to determine dynamic stiffness and phase angle as a function of frequency [15,43]. The dynamic stiffness characterizes the dynamic modulus of the material, while the phase angle describes the energy dissipation characteristics.

Specimen preparation

Five pairs of human MCLs were used in this study (53.6 ± 10.3 yrs, 3 males, 2 female). Donor knees were allowed to thaw at room temperature for 12 h prior to dissection. At the time of dissection, no signs of arthritis or previous soft tissue injury were found in any of the knees. The right or left MCL was chosen at random for harvest of a specimen for longitudinal tensile testing along the fiber direction (referred to herein as the longitudinal test). Test specimens for tensile testing transverse to the predominant collagen fiber direction (the transverse test) and shear testing along the fiber direction (the shear test) were harvested from the contralateral ligament. A hardened steel punch in the shape of a dumbbell test specimen (2 mm wide with 14 mm clamp-to-clamp distance, aspect ratio 7:1) was used to harvest the longitudinal test specimen from the anterior edge of the superficial MCL, distal to the medial meniscus and proximal to the beginning of the tibial insertion of the MCL [35] (Fig. 1). A different dumbbell-shaped steel punch (gauge dimensions 4 mm wide with 11 mm clamp-to-clamp distance, aspect ratio 2.75:1) was used to harvest a transverse test specimen. A rectangular 10 × 25 mm hardened steel punch was used to harvest samples for shear testing [45]. Transverse and shear specimens were harvested from the anterior region of the superficial MCL (Fig. 1). The ends of each test specimen were wrapped in saline soaked gauze and the specimen was mounted in a pair of custom clamps [35]. Digital calipers were used to measure the initial distance

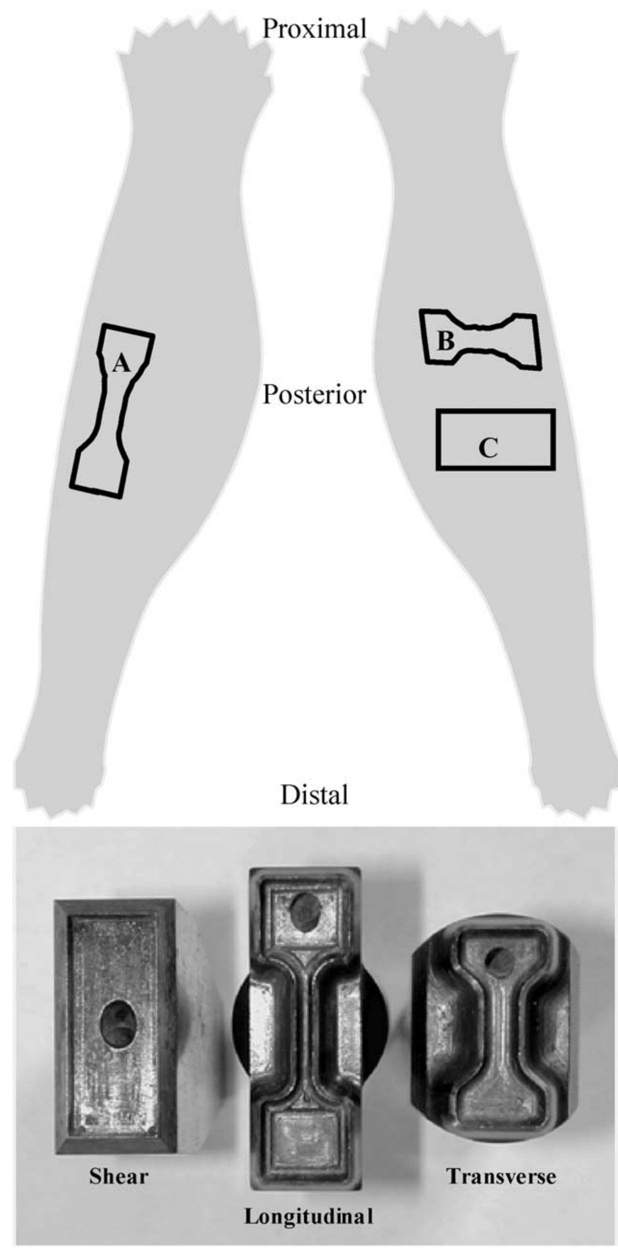

Fig. 1. Top—schematic illustrating harvest locations for (A) longitudinal, (B) transverse and (C) shear test specimens for a left–right pair of MCLs. Bottom—hardened steel punches used to harvest the test specimens.

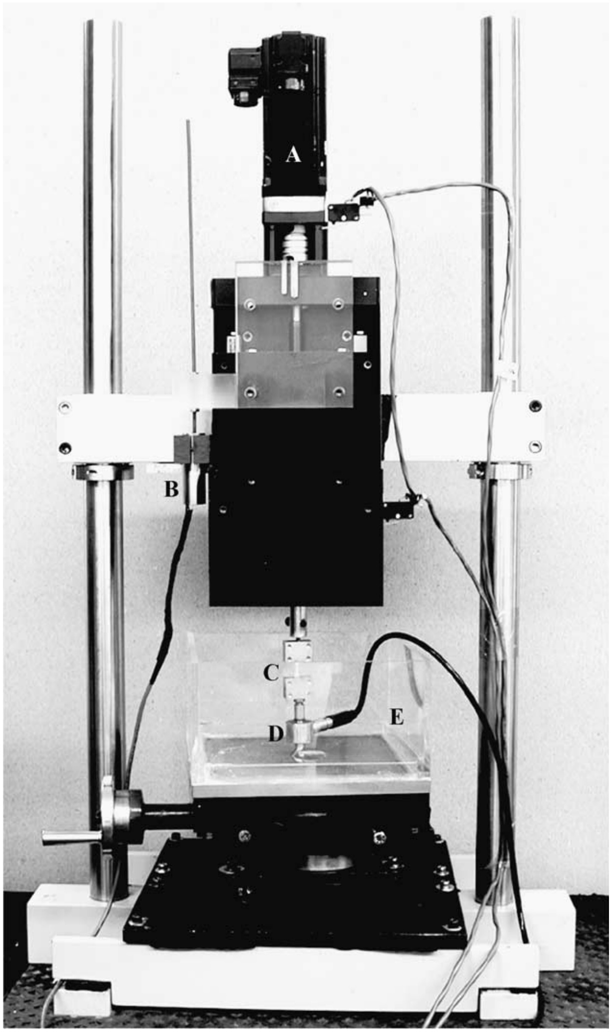

Fig. 2. Custom designed material testing machine. (A) Computer-controlled servomotor, (B) linear variable differential transformer (LVDT), (C) test specimen, (D) waterproof load cell, and (E) chamber. The top of the chamber used to enclose the tissue sample is not shown. A tube through the top of the chamber was connected to a humidifier system that pumped warm humidified air into the chamber.

between the clamps and the width and thickness of the sample halfway between the clamps. Each measurement was taken three times and averaged, and cross-sectional area was calculated by assuming a rectangular shape. All tests were performed inside an environmental chamber that maintained a constant temperature of 37 °C and 100% humidity, using a custom designed tensile test machine (Fig. 2).

Two black contrast markers (1.5 mm dia.) were adhered to the central third of the longitudinal and transverse specimens using cyanoacrylate. The markers were recorded during testing using a digital camera (Pulnix TM-1040, 1024×1024×30 fps, Sunnyvale, CA) and framegrabber (Bitflow Roadrunner, Woburn, MA). Load was monitored with a 22 N waterproof load cell for longitudinal tests and a 4.9 N waterproof load cell for shear and transverse tests (accuracies ±0.05% of full-scale load, Sensotec Inc, Columbus, OH). Elongation was monitored with a linear variable differential transformer (LVDT) (Schaevitz, Hampton, VA). Load and elongation data were collected at 500 Hz.

Test protocol

Testing consisted of incremental stress relaxation tests followed by sinusoidal cyclic testing at a series of oscillation frequencies. Parameters for the longitudinal, transverse and shear test configurations were optimized during a large series of preliminary tests to ensure that (1) relaxation times were sufficiently long to allow equilibrium to be achieved at each strain level, (2) equilibrium strain levels were within the expected operating range of the tissue but below the failure levels, and (3) tissue response to oscillatory strain was linear (Table 1). In other words, when a sinusoidal strain–time input was applied, the resulting stress–time signal was well described by a sine wave and the positive and negative portions of the signal amplitude were nearly identical about the equilibrium stress level.

For longitudinal and transverse tests, the zero-load length was established by consecutively applying and removing a small tare load. Preconditioning was performed by stretching the sample at 1%/s to the strain levels indicated in Table 1 (clamp-to-clamp strain) and allowing the specimen to stress-relax for 10 min. This was followed by a 10-min recovery period. The preconditioning strain levels were chosen to just exceed the maximum clamp-to-clamp strains experienced by the samples during the entire test sequence [42]. The zero-load length was then re-established. This was followed by incremental stress relaxation tests and sinusoidal cyclic loading. Specimens were stretched to the first equilibrium strain level in Table 1 at 1%/s, allowed to stress-relax for the times indicated, and then subjected to sinusoidal oscillations at six different oscillation frequencies spanning over two decades. After completion, the entire protocol was repeated at the two higher equilibrium strain levels. Finally, for a subset of the samples, the stress relaxation and cyclic testing were repeated at the lowest strain level to ensure that the response was repeatable and not dependent on the order of the tests.

Data reduction and statistical analysis

Peak and equilibrium engineering stresses (first Piola–Kirchhoff stresses, F/A_0, where F is the current force and A_0 is the initial cross-sectional area) [41] were determined for the stress relaxation tests at each strain level. The tissue engineering strains ($(l - l_0)/l_0$, where l is the current length and l_0 is the reference length) were determined from the digital camera data obtained during relaxation at each strain level. These data were used to generate stress–strain curves. The stress–time curves from the stress relaxation tests were normalized by the peak stress to obtain reduced relaxation curves [17]. A two-factor repeated measures ANOVA was used to test for the effects of strain level and time (0.1, 10.0 and 1000.0 s) for each test configuration. Data from the highest strain level were used to determine the effects of test

Table 1
Parameters used for the different test configurations

	Longitudinal			Transverse			Shear		
Tare load (N)		0.49			0.20			N/A	
Precond. level (%)		8.5			18			49	
Equil strains (%)	4	6	8	8	12	16	25	35	45
Tissue strains (%)	1.6 ± 0.7	2.4 ± 1.1	3.2 ± 1.5	3.8 ± 1.3	5.9 ± 1.9	7.5 ± 3.0	N/A	N/A	N/A
Relax. time (min)	25	40	55	20	25	30	10	20	30
Osc. strain (%)		±0.125			±0.500			±1.000	
Osc. freq. (Hz)	0.01, 0.1, 1.0, 5.0, 10.0, 15.0			0.01, 0.1, 1.0, 5.0, 10.0, 15.0			0.01, 0.1, 1.0, 3.0, 5.0, 10.0		

configuration and time with a two-factor repeated measures ANOVA. When significance was detected ($p \leqslant 0.05$), Tukey tests were performed between different levels of a factor.

Cyclic load–time curves were converted to stress–time curves by dividing the load by the cross-sectional area. For longitudinal and transverse tests, engineering tissue strains were calculated from measurements of the lengths between the fiducial markers. Because the digital camera could only record at 30 Hz, the relationship between clamp-to-clamp strain and tissue strain for the longitudinal and transverse cyclic testing was established using tissue strains measured during cyclic testing at 0.1 Hz. This yielded the amplitude of the strain–time signal A_ε in terms of tissue strain. For the shear tests, shear strain, $\tan(\theta)$, was calculated based on the specimen width and crosshead displacement [18,45]:

$$\tan(\theta) = \frac{\text{crosshead displacement}}{\text{initial width}}. \tag{1}$$

The cyclic strain–time and stress–time data were fit to a four-parameter sine function:

$$y = y_0 + A\sin\left(\frac{2\pi t}{b} + \phi\right). \tag{2}$$

Here, y and t represent the strain (or stress) and time data, respectively, y_0 represents the equilibrium strain (or stress) level and A denotes the amplitude of the sine wave. ϕ represents the phase and b denotes the inverse of the frequency (1/Hz). Dynamic stiffness M (Pascals) and phase angle ϕ (radians) were calculated for each equilibrium strain level and frequency:

$$M = \frac{A_\sigma}{A_\varepsilon}; \qquad \phi = \phi_\sigma - \phi_\varepsilon. \tag{3}$$

A_σ and A_ε denote the amplitudes of the cyclic stress–time and strain–time data, respectively, while ϕ_σ and ϕ_ε denote the corresponding phase angles [15].

A two-factor repeated measures ANOVA was used to test for the effects of strain level and oscillation frequency on the dynamic stiffness and phase for each test configuration. Dynamic stiffness and phase data from the highest strain level were used to determine the effects of test configuration and frequency with a two-factor repeated measures ANOVA, using the frequencies that were common to all three tests (0.01, 0.1, 1.0, 5.0, 10.0 Hz). When significance was detected ($p \leqslant 0.05$), Tukey tests were performed between different levels of a factor.

Results

Peak and equilibrium stress–strain curves

Peak and equilibrium stresses for longitudinal tests were up to 200 times larger than those for transverse and shear tests (Fig. 3). The longitudinal and shear stress–strain curves demonstrated the largest nonlinearity, while the transverse stress–strain curves were relatively linear. As expected, the material tangent modulus was lowest under shear loading. Tissue strains were approximately half the measured clamp-to-clamp strains for the longitudinal and transverse stress relaxation tests, yet a highly linear relationship was obtained between the clamp strain and tissue strain for all tensile tests (average correlation coefficient across all longitudinal and transverse tests: $R^2 = 0.996 \pm 0.011$). Repeat of the testing at the lowest strain level demonstrated that the viscoelastic response was not dependent on the order of the tests. There was very little variation in cross-sectional area measurements between samples (Table 2).

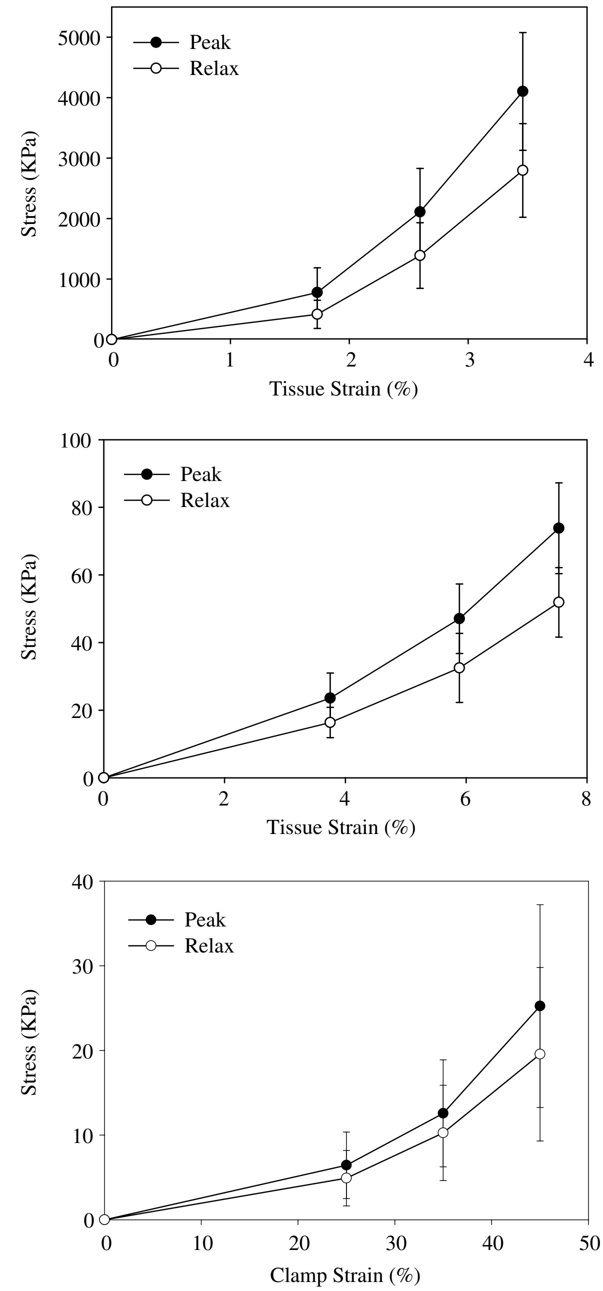

Fig. 3. Peak and equilibrium stress vs. strain (mean ± standard deviation) obtained during the incremental stress relaxation tests for longitudinal (top), transverse (middle) and shear (bottom) tests. Data for the longitudinal and transverse tests are in terms of tissue strain, while data for the shear test are in terms of clamp strain. Note the different scales for the three plots.

Reduced relaxation curves

Although peak and equilibrium stresses differed dramatically in magnitude under the different test configurations, there were comparable amounts of percent relaxation (Fig. 4). The largest percent relaxation was observed for the longitudinal tests at the lowest strain level. Relaxation proceeded faster at the lowest strain

Table 2
Dimensions of the MCL test specimens (mean ± standard deviation)

Specimen type	Initial length (mm) before preconditioning	Initial length (mm) after preconditioning	Width (mm)	Thickness (mm)
Longitudinal	12.9 ± 0.6	13.2 ± 0.6	2.3 ± 0.1	1.5 ± 0.2
Transverse	5.9 ± 0.7	6.1 ± 0.8	4.3 ± 0.2	1.6 ± 0.4
Shear	10.2 ± 0.3	N/A	7.6 ± 0.9	1.7 ± 0.9

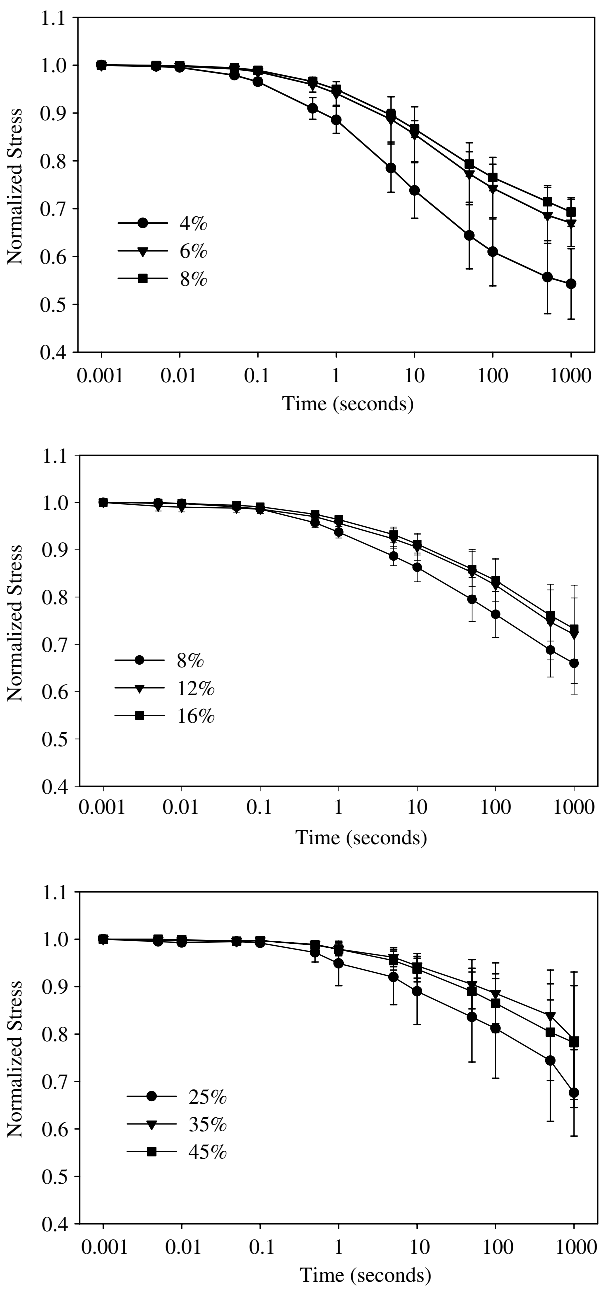

Fig. 4. Reduced stress relaxation curves for longitudinal (top), transverse (middle) and shear tests (bottom). Legends indicate applied clamp-to-clamp strain. Mean ± standard deviation.

level for all three test configurations, while the reduced relaxation curves for the two higher strain levels were nearly indistinguishable. There was a significant effect of strain level on the reduced relaxation values for all three test configurations ($p = 0.001$, $p < 0.001$ and $p = 0.016$ for longitudinal, transverse and shear tests). Multiple comparisons revealed that the data for the lowest strain level were significantly lower than the two higher strain levels for all three tests, while there was no significant difference between results for the middle and highest strain levels. The reduced relaxation curves obtained from the incremental stress relaxation tests exhibited two separate slopes. There was no effect of test type on the reduced relaxation curves.

Cyclic testing

There was a significant increase in the dynamic stiffness M as a function of strain level for all three tests ($p < 0.01$ for all cases), indicating that the modulus of the material depends on the strain level (Fig. 5, left column). For the longitudinal tests, M at 4% clamp-to-clamp strain was significantly less than that at 6% and 8%. For the transverse tests, M was significantly greater at 16% clamp-to-clamp strain than at 8%. For the shear tests, M was significant greater at 45% shear strain than at 25% and 35% strain. Although not readily apparent in the graphs (Fig. 5), there was a significant effect of frequency on M for longitudinal and shear tests ($p < 0.0001$ and $p = 0.013$, respectively). For the longitudinal tests, the dynamic stiffness at 15 Hz was significantly greater than 5, 0.1 and 0.01 Hz, the dynamic stiffness at 10 Hz was significant greater than at 0.01 and 0.1 Hz, the dynamic stiffness at 1 Hz was significantly greater than at 0.01 Hz, and the dynamic stiffness at 5 Hz was significantly great than at 0.01 Hz. For the shear tests, M was significantly greater at 10 Hz than at 0.1 Hz. There was a significant interaction between strain and frequency on the dynamic stiffness for the longitudinal and shear tests ($p < 0.001$ and $p = 0.002$, respectively).

The change in phase angle ϕ with frequency was similar in magnitude and shape for all three test configurations. Lower positive values describe less material damping, indicative of solid behavior, while higher values indicate a more viscous behavior. There was a significant effect of frequency on ϕ for all three test configurations ($p < 0.001$ in all cases) (Fig. 5, right column). For all three test configurations, the phase angle showed a marked increase above 1 Hz. For all

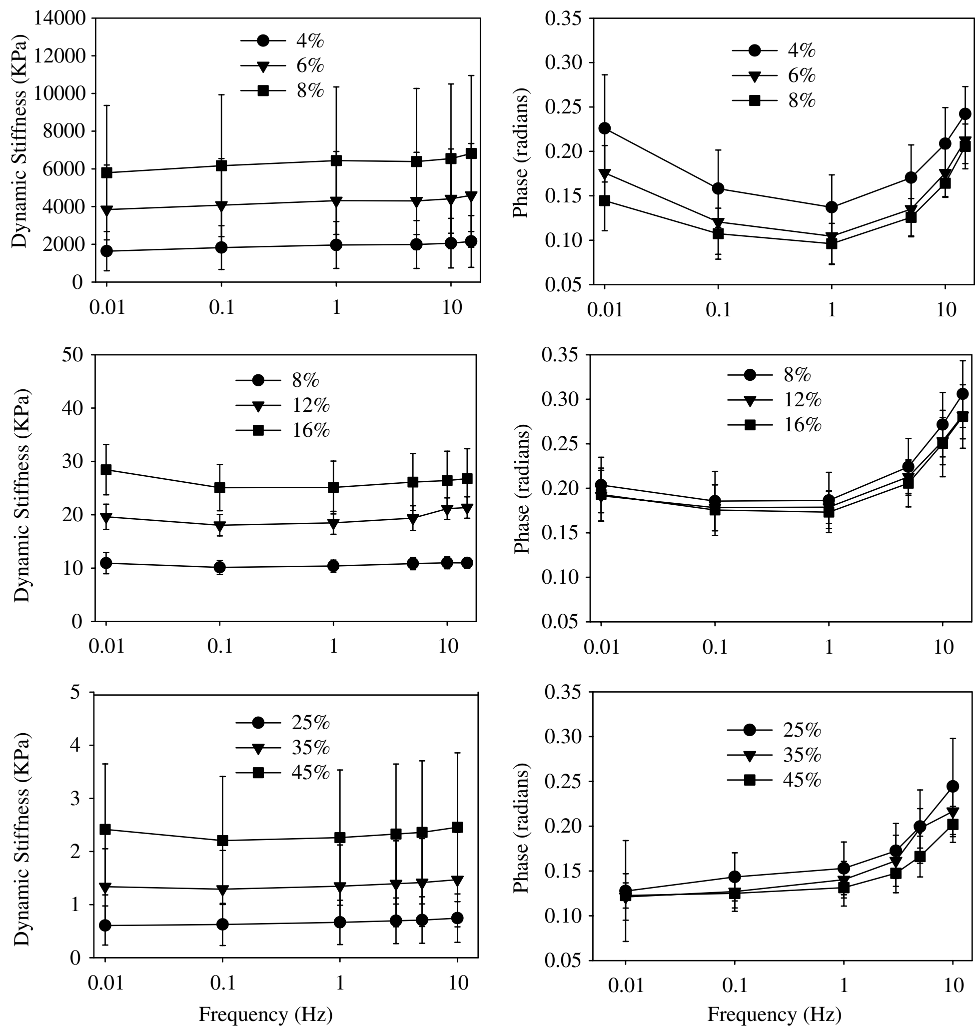

Fig. 5. Dynamic stiffness (left column) and phase angle (right column) as a function of oscillation frequency and strain amplitude for longitudinal (top row), transverse (middle row) and shear (bottom row) test configurations. Legends indicate applied clamp-to-clamp strain. Dynamic stiffness for the longitudinal and transverse tests is presented in terms of measured tissue strain. Mean ± standard deviation.

three tests, the phase at 10 and 15 Hz was significantly greater than all lower frequencies. In the case of the longitudinal tests, the phase at 0.01 Hz was significantly greater than that at 0.1, 1.0 and 10.0 Hz. Only the longitudinal test showed a significant effect of strain level on phase angle ($p = 0.005$), with the lowest strain level exhibiting a larger phase angle than the higher strain levels. There was a significant interaction between strain level and frequency for the longitudinal phase data ($p = 0.006$).

Comparisons between test types at the highest strain levels revealed significant differences in dynamic stiffness but not phase angle. There was a significant effect of test type on the dynamic stiffness ($p = 0.001$), with the longitudinal test demonstrating significantly higher dynamic stiffness than both the transverse and shear tests. The phase angle was unaffected by the type of test. There was a significant effect of frequency on both the dynamic stiffness and phase angle ($p < 0.001$ in both cases).

Discussion

This study quantified the viscoelastic material behavior of human MCLs under incremental stress relaxation and oscillatory loading. A custom test device and a detailed experimental protocol were developed to study the viscoelastic response of the tissue under three different test configurations. Incremental stress relaxation tests revealed that relaxation occurred faster at the lowest strain levels for all three tests. The dynamic stiffness increased with strain level for all three tests, while there was a significant effect of frequency on the dynamic stiffness for only the longitudinal and shear test configurations. The magnitude of the dynamic stiffness varied greatly with test mode but the qualitative behavior was very similar between test modes. Results showed an increase of phase angle with frequency, indicating that the tissue is more effective at dissipating energy at higher strain rates.

The peak and equilibrium stress–strain curves provide insight into the ultrastructural features of the tissue that resist stretch and shear. The toe region of the longitudinal stress–strain curves has been attributed to the uncrimping of collagen (Fig. 3, top panel) [13,20,24,44]. However, the shear and transverse stress–strain curves were also nonlinear (Fig. 3, middle and bottom panels) [45]. The stress–strain response of the tissue to transverse tensile loading and along-fiber shear stress–strain curves may have contributions from interfibrillar and/or intermolecular crosslinks [9,12,31,34,36]. The presence of intermolecular crosslinks is an important determinant of tendon longitudinal stress–strain behavior. An increased number of intermolecular crosslinks corresponds with an increased tissue modulus [3,12,14] while a decrease due to treatment with beta-aminopropionitrile reduces tissue modulus in a dose-dependent fashion [27,34]. Interfibrillar crosslinks are arranged orthogonally across the collagen fibrils at the "D" band in the gap zone between fibrils [40], and this relative orientation does not change under uniaxial tensile loading in tendons [9]. This suggests that the resistance of interfibrillar crosslinks to loading would be maximized during stretching transverse to the fibril direction, while shear and tensile loading would tend to shear the collagen fibrils relative to each other, thus stretching interfibrillar crosslinks but to a lesser extent. A model of interfibrillar crosslinking via glycosaminoglycans demonstrated that such a geometric arrangement does in fact give rise to nonlinear load–elongation behavior when fibrils are sheared with respect to each other [36]. However, this study assumed that the loading of the crosslinks was due to relative motion of the fibrils under tensile loading, causing shearing of the crosslinks. Cribb and Scott have demonstrated that the orientation of the crosslinks is unchanged during tensile loading [9]. Thus, it would seem more likely that interfibrillar crosslinks resist loading that results in relative displacement of the fibrils. Both intermolecular and interfibrillar crosslinks could potentially contribute to the elastic and viscoelastic response of ligament under the loading conditions examined in this study, and the test protocol used in this study could be used to investigate the effects of chemical treatment and/or diet, which can modify interfibrillar and intermolecular crosslinks, respectively.

The normalized incremental stress relaxation curves provide insight into the time- and strain-level dependent viscoelasticity of the MCL. The relaxation curves obtained from all three test configurations were very similar to each other. Incremental stress relaxation proceeded faster at the lowest strain levels for all three test configurations. Relaxation under strain along the longitudinal direction occurs more quickly at lower strain levels in rat MCLs, and the effect of strain level becomes less significant at strains that reflect the end of the toe region [32]. The authors suggested that water loss could be increased at higher strains, resulting in a more elastic response during stress relaxation. Another possibility is that the ground substance matrix bears a larger percentage of load at lower strains due to the fact that the collagen fibers are still crimped, and the increased amount of relaxation is related to the viscous nature of the ground substance matrix (i.e., proteoglycans, crosslinks).

The normalized stress relaxation curves exhibited one slope over the time range from 0.0 to 0.1 s, and a second, steeper slope following that time (Fig. 4). In linear viscoelasticity theory, each linear region corresponds to a separate relaxation mechanism (i.e., a separate Kelvin model with a distinct relaxation time for each slope) [43]. Most of the reduced relaxation curves reported in the literature for soft tissue exhibit only a single slope when plotted with semi-log axes. However, close examination of the data revealed that these studies did not report the short-time data. Clineff et al. [8] reported the reduced relaxation functions for both normal and healing goat MCL were linear, but this study used data from 6 s on to determine the relaxation curves. Abramowitch et al. [1] found similar results for the goat MCL, but only data from about 3 s on were used. Kwan et al. [26] reported the reduced relaxation function for porcine anterior cruciate ligaments. The results are very similar to our longitudinal relaxation curves for the long-term relaxation behavior (Fig. 5).

The dynamic stiffness of human MCL varied greatly with test mode and equilibrium strain level, while the magnitude showed a small but significant increase with increasing oscillation frequency (Fig. 5). The increases in dynamic stiffness with strain level for all three test configurations can be partially explained by the elastic stress–strain behavior presented in Fig. 3 [35,45]. The strain-dependent dynamic stiffness is a nonlinear viscoelastic phenomenon, but it can still be described within the context of quasilinear viscoelasticity (see, e.g., [17]). The small but significant increase in dynamic stiffness with frequency is consistent with other reports of small but significant increases in ligament tangent modulus and stiffness with increasing strain rate [10,11].

The phase angle had remarkably similar magnitudes and variation with frequency across all three test configurations. The only exception was the higher phase angle at low frequencies for the longitudinal tests. Phase was unaffected by strain level, with exception of the lowest strain level for the longitudinal tests. This result is consistent with the incremental stress relaxation data and may be due to an energy dissipation mechanism that is active when the collagen fibers are still crimped. The increase in phase at higher frequencies implies increased energy dissipation, which may provide a protective mechanism under fast loading. A similar trend was noted for the phase angle of human lumbar nucleus pulposus [25]. This effect cannot be described by the standard quasilinear viscoelastic theory [17,33], which predicts a nearly constant phase over a wide range of frequencies.

The test protocol for viscoelastic characterization was specifically designed to allow for both incremental stress relaxation testing and sinusoidal testing at multiple levels of strain. Although incremental stress relaxation testing has been used to characterize the time-dependent material properties of other soft tissues such as articular cartilage [30] and skin [37], it has not been used for characterization of ligament and tendons. Thus, care must be taken when comparing the results of the present incremental relaxation tests with studies that performed relaxation tests at different strain levels but started each test at the zero-load length of the tissue (e.g., [32]). The amount of relaxation between, for instance, the second and third strain levels is less than would be expected if the tissue were stretched from the strain-free configuration to the third strain level directly. This study also used a preconditioning strain level that was higher than the maximum applied strain during the entire test sequence. This approach was adopted because preconditioning is an irreversible, strain-level dependent phenomenon in tendons [22], and the effects of preconditioning are independent of inherent viscoelastic material properties [42]. The test order and repeatability of the data is also worthy of mention. We verified the lack of an effect of the strain history by re-testing the specimens at the lowest strain level. It is of course possible that there could have been differences if the tests were also repeated at the higher strain levels. Preliminary testing showed that relaxation proceeded fastest at the lowest strains, and the tests were repeated at the lowest strain level with the thought that results would be most sensitive to the test history at the lower strain levels. Finally, it should be mentioned that the aspect ratio for the transverse specimens (2.75:1) is somewhat less than ideal for a uniaxial tensile test. This may have resulted in some resistance to lateral contraction at the center of the sample. For the transverse test configuration, the anatomical dimensions of the MCL in the transverse direction limited the length of the test specimen.

When comparing results from different test configurations, it was tacitly assumed that the MCL was homogeneous and that there were minimal left–right differences in the tissue. Due to the size and geometry of the MCL, three samples (longitudinal, transverse and shear) could not be extracted from the same ligament. The superficial MCL has a highly organized structure of parallel collagen fibers connecting the femoral and tibial insertions along approximately the anterior two thirds. The posterior third of the MCL sometimes contains less organized and possibly a lower density of collagen fibers. Further, the density of collagen in knee ligaments is inhomogeneous [29]. As a result, the use of test samples from different tissue locations may introduce additional error into comparisons between test configurations. There were no apparent visual differences between paired MCLs from the same donor. This approach was justified by the desire to obtain three test samples from the same donor.

Measured tissue strains were approximately half of the applied clamp strains for longitudinal and transverse tests. Discrepancies between clamp strains and tissue strains have been analyzed systematically [5]. Local deformation due to tissue clamping causes higher strains near the clamps, yielding lower strains in the tissue midsubstance. In the present study, this occurred despite the fact that dumbbell-shaped test specimens were used. Further, it has been suggested that differences between clamp strain and tissue strain may also be related to the relative sliding of collagen fibrils [16,34,36]. To minimize the potential influence of strain inhomogeneity on the calculations, tissue strain measurements were performed using markers placed in the central third of the sample for longitudinal and transverse tests. A highly linear relationship was obtained between the clamp strain and tissue strain for all tensile tests, supporting the idea that the strain distribution in the measurement region was homogeneous.

Special care must be taken when interpreting the results of the shear tests. The shear test configuration produces an inhomogeneous strain field in the test sample [18,45]. Thus, the reported stresses and strains must be considered "average" values. An alternative approach to analyzing the data from the shear tests involves finite element modeling of each test specimen to capture the inhomogeneous strain field, and then using a parameter optimization approach to determine the best set of material parameters for a constitutive model [45]. However, this approach would first require the definition of an appropriate viscoelastic constitutive model to represent all of the experimental data, and this constitutive model would have to be implemented in a finite element code.

Although the theory of linear viscoelasticity was used to analyze the data at each strain level and frequency, this does not limit the interpretation of the data to the linear theory. The effects of strain level reveal the nonlinear response of the tissue. Strain amplitudes were carefully chosen to ensure a linear response at each strain level. The use of larger amplitudes of strain input resulted in a stress–time curve that was no longer faithfully represented by a sine wave. Strain amplitudes were chosen to be as small as possible while still maintaining an acceptable signal/noise ratio in the load cell output. The use of the linear theory allows a systematic investigation of tissue viscoelastic response and thus points to further experiments that can be devised to characterize nonlinear aspects of the material behavior. Further experiments of the nonlinear response can be conducted using the same experimental protocol with larger strain amplitudes. However, analysis and interpretation of the resulting data are considerably more complicated.

In summary, the data reported in this study provide insight into the anisotropic viscoelastic material properties of ligament. The peak and equilibrium stress–strain curves for the longitudinal, transverse and shear tests demonstrate that the instantaneous and long-time stress–strain response of the tissue differs significantly between loading conditions of along-fiber stretch, cross-fiber stretch and along-fiber shear. The reduced relaxation functions had at least two distinct slopes on a log-linear plot for all three test modes. Normalized stress relaxation curves were unaffected by strain level with exception of lowest strain level for longitudinal samples, and phase was unaffected by strain level with exception of lowest strain level for longitudinal samples. This suggests that the viscoelastic response of the tissue is affected by the state of crimp in the collagen fibers. Overall, the results of this study suggest that the long-time relaxation behavior of the medial collateral ligament and the short-time dynamic energy dissipation of the human medial collateral ligament may be governed by either different viscoelastic mechanisms or a response that evolves with changes in collagen fiber strain level, yet the tissue viscoelasticity under different loading configurations is similar. These data will allow the formulation and validation of three-dimensional constitutive models that account for material anisotropy and dynamic viscoelastic behavior of ligaments, providing a means to accurately describe and predict stress and strain under viscoelastic loading conditions.

Acknowledgements

Financial support from NIH grant #AR47369 is gratefully acknowledged. The authors thank Ben Ellis for his assistance with design and construction of the test system.

References

[1] Abramowitch SD, Woo SL, Clineff TD, Debski RE. An evaluation of the quasi-linear viscoelastic properties of the healing medial collateral ligament in a goat model. Ann Biomed Eng 2004;32(3):329–35.
[2] Atkinson TS, Haut RC, Altiero NJ. A poroelastic model that predicts some phenomenological responses of ligaments and tendons. J Biomech Eng 1997;119:400–5.
[3] Bailey AJ, Paul RG, Knott L. Mechanisms of maturation and ageing of collagen. Mech Ageing Dev 1998;106:1–56.
[4] Bailey AJ, Robins SP, Balian G. Biological significance of the intermolecular crosslinks of collagen. Nature 1974;251:105–9.
[5] Butler DL, Grood ES, Noyes FR, Zernicke RF, Brackett K. Effects of structure and strain measurement technique on the material properties of young human tendons and fascia. J Biomech 1984;17:579–96.
[6] Butler SL, Kohles SS, Thielke RJ, Chen C, Vanderby Jr R. Interstitial fluid flow in tendons or ligaments: a porous medium finite element simulation. Med Biol Eng Comput 1997;35: 742–6.
[7] Chimich D, Shrive N, Frank C, Marchuk L, Bray R. Water content alters viscoelastic behaviour of the normal adolescent rabbit medial collateral ligament. J Biomech 1992;25:831–7.
[8] Clineff TD, Debski RE, Scheffler SU, Woo SL, 1999. Experimental & theoretical evaluation of the viscoelastic properties of the healing goat medial collateral ligament. Presented at Bioengineering Conference ASME.
[9] Cribb AM, Scott JE. Tendon response to tensile stress: an ultrastructural investigation of collagen:proteoglycan interactions in stressed tendon. J Anat 1995;187:423–8.
[10] Crisco JJ, Moore DC, McGovern RD. Strain-rate sensitivity of the rabbit MCL diminishes at traumatic loading rates. J Biomech 2002;35:1379–85.
[11] Danto MI, Woo SL. The mechanical properties of skeletally mature rabbit anterior cruciate ligament and patellar tendon over a range of strain rates. J Orthop Res 1993;11:58–67.
[12] Davison PF. The contribution of labile crosslinks to the tensile behavior of tendons. Connect Tissue Res 1989;18:293–305.
[13] Diamant J, Keller A, Baer E, Litt M, Arridge RGC. Collagen; ultrastructure and its relation to mechanical properties as a function of ageing. Proc R Soc London, Ser B Biol Sci 1972;180: 293–315.
[14] Eyre DR, Paz MA, Gallop PM. Cross-linking in collagen and elastin. Annu Rev Biochem 1984;53:717–48.
[15] Findley W, Lai J, Onaran K. Creep and relaxation of nonlinear viscoelastic materials, with an introduction to linear viscoelasticity. Amsterdam: North Holland Publishing Co; 1976.
[16] Fratzl P, Misof K, Zizak I, Rapp G, Amenitsch H, Bernstorff S. Fibrillar structure and mechanical properties of collagen. J Struct Biol 1998;122:119–22.
[17] Fung YC. Biomechanics: mechanical properties of living tissues. New York: Springer-Verlag; 1993.
[18] Gardiner JC, Weiss JA. Simple shear testing of parallel-fibered planar soft tissues. J Biomech Eng 2001;123:170–5.
[19] Gardiner JC, Weiss JA, Rosenberg TD. Strain in the human medial collateral ligament during valgus loading of the knee. Clin Orthop 2001:266–74.
[20] Hansen KA, Weiss JA, Barton JK. Recruitment of tendon crimp with applied tensile strain. J Biomech Eng 2002;124:72–7.
[21] Haut RC. The effect of a lathyritic diet on the sensitivity of tendon to strain rate. J Biomech Eng 1985;107:166–74.
[22] Hubbard RP, Chun KJ. Mechanical responses of tendons to repeated extensions and wait periods. J Biomech Eng 1988;110: 11–9.
[23] Hull ML, Berns GS, Varma H, Patterson HA. Strain in the medial collateral ligament of the human knee under single and combined loads. J Biomech 1996;29:199–206.
[24] Hurschler C, Provenzano PP, Vanderby Jr R. Scanning electron microscopic characterization of healing and normal rat ligament microstructure under slack and loaded conditions. Connect Tissue Res 2003;44:59–68.
[25] Iatridis JC, Setton LA, Weidenbaum M, Mow VC. The viscoelastic behavior of the non-degenerate human lumbar nucleus pulposus in shear. J Biomech 1997;30:1005–13.
[26] Kwan MK, Lin TH, Woo SL. On the viscoelastic properties of the anteromedial bundle of the anterior cruciate ligament. J Biomech 1993;26:447–52.
[27] Lees S, Eyre DR, Barnard SM. BAPN dose dependence of mature crosslinking in bone matrix collagen of rabbit compact bone: corresponding variation of sonic velocity and equatorial diffraction spacing. Connect Tissue Res 1990;24:95–105.

[28] Miyasaka KC, Daniel DM, Stone ML, Hirshman P. The incidence of knee ligament injuries in the general population. Am J Knee Surg 1991;4:3–8.

[29] Mommersteeg TJ, Blankevoort L, Kooloos JG, Hendriks JC, Kauer JM, Huiskes R. Nonuniform distribution of collagen density in human knee ligaments. J Orthop Res 1994;12:238–45.

[30] Mow VC, Kuei SC, Lai WM, Armstrong CG. Biphasic creep and stress relaxation of articular cartilage in compression: theory and experiments. J Biomech Eng 1980;102:73–84.

[31] Patterson-Kane JC, Parry DA, Birch HL, Goodship AE, Firth EC. An age-related study of morphology and cross-link composition of collagen fibrils in the digital flexor tendons of young thoroughbred horses. Connect Tissue Res 1997;36:253–60.

[32] Provenzano P, Lakes R, Keenan T, Vanderby Jr R. Nonlinear ligament viscoelasticity. Ann Biomed Eng 2001;29:908–14.

[33] Puso MA, Weiss JA. Finite element implementation of anisotropic quasilinear viscoelasticity. J Biomech Eng 1998;120:62–70.

[34] Puxkandl R, Zizak I, Paris O, Keckes J, Tesch W, Bernstorff S, et al. Viscoelastic properties of collagen: synchrotron radiation investigations and structural model. Philos Trans R Soc London, Ser B Biol Sci 2002;357:191–7.

[35] Quapp KM, Weiss JA. Material characterization of human medial collateral ligament. J Biomech Eng 1998;120:757–63.

[36] Redaelli A, Vesentini S, Soncini M, Venab P, Mantero S, Montevecchi FM. Possible role of decorin glycosaminoglycans in fibril to fibril force transfer in relative mature tendons—a computational study from molecular to microstructural level. J Biomech 2003;36:1555–69.

[37] Reihsner R, Menzel EJ. Two-dimensional stress-relaxation behavior of human skin as influenced by non-enzymatic glycation and the inhibitory agent aminoguanidine. J Biomech 1998;31:985–93.

[38] Rubin MB, Bodner SR. A three-dimensional nonlinear model for dissipative response of soft tissue. Int J Solids Struct 2002;39: 5081–99.

[39] Scott JE. Structure and function in extracellular matrices depend on interactions between anionic glycosaminoglycans. Pathol Biol (Paris) 2001;49:284–9.

[40] Scott JE, Orford CR. Dermatan sulphate-rich proteoglycan associates with rat tail-tendon collagen at the d band in the gap region. Biochem J 1981;197:213–6.

[41] Spencer AJM. Continuum mechanics. New York, 1980.

[42] Sverdlik A, Lanir Y. Time-dependent mechanical behavior of sheep digital tendons, including the effects of preconditioning. J Biomech Eng 2002;124:78–84.

[43] Tschoegl NW. The phenomenological theory of linear viscoelastic behavior. New York: Springer-Verlag; 1989.

[44] Viidik A, Ekholm R. Light and electron microscopic studies of collagen fibers under strain. Z Anat Entwickl Gesch 1968;127:154–64.

[45] Weiss JA, Gardiner JC, Bonifasi-Lista C. Ligament material behavior is nonlinear, viscoelastic and rate-independent under shear loading. J Biomech 2002;35:943–50.

[46] Yamamoto E, Hayashi K, Yamamoto N. Effects of stress shielding on the transverse mechanical properties of rabbit patellar tendons. J Biomech Eng 2000;122:608–14.